

# *N*-acetylglucosaminyltransferase IVa regulates metastatic potential of mouse hepatocarcinoma cells through glycosylation of CD147

Jianhui Fan · Shujing Wang · Shengjin Yu · Jingna He · Weilong Zheng · Jianing Zhang

Received: 12 April 2012 / Revised: 4 June 2012 / Accepted: 5 June 2012 / Published online: 27 June 2012  
© Springer Science+Business Media, LLC 2012

**Abstract** *N*-acetylglucosaminyltransferase (GnT)-IV a is a key enzyme that catalyzes the formation of the GlcNAc  $\beta$ 1-4 branch on the core structure of complex N-Glycans, which is the common substrate for other *N*-acetylglucosaminyltransferases, such as GnT-III and GnT-V. Our recent study indicates that the expression of GnT-IVa in Hca-F cells was much higher than that in Hepal-6 cells, these two mouse hepatocarcinoma cell lines have high and no metastatic potential in lymph nodes respectively. To investigate the effects of GnT-IVa on the metastasis of hepatocarcinoma, exogenous GnT-IVa was introduced into Hepal-6 cells, and on the other hand, the expression of GnT-IVa was down-regulated in Hca-F cells. The engineered overexpression of GnT-IVa in Hepal-6 cells increased the antennary branches of complex N-glycans and reduced bisecting branches *in vitro* and *in vivo*, which leads to the increase in migration and metastatic capability of hepatocarcinoma cells. Conversely, down-regulated expression of GnT-IVa in Hca-F cells showed reduced tetra-antennary branches of N-Glycans, and significantly decreased the migration and metastatic capability. Furthermore, we found that the regulated GnT-IVa converts the heterogeneous N-glycosylated forms of CD147 in Hepal-6 and Hca-F cells, and significantly changed the antennary oligosaccharide structures on CD147. These results suggest that GnT-IVa could be acting as a key role in migration and metastasis of mouse hepatocarcinoma cells through altering the glycosylation of CD147. These findings

should be valuable in delineating the important function of GnT-IVa during the process of hepatocarcinoma growth and metastasis.

**Keywords** *N*-acetylglucosaminyltransferase-IVa (GnT-IVa) · N-Glycans · Hepatocarcinoma · Cell Migration · CD147

## Abbreviations

GnT	<i>N</i> -acetylglucosaminyltransferase
<i>Mgat4</i>	Mannoside acetylglucosaminyltransferase 4
GAPDH	Glyceraldehyde phosphate dehydrogenase
L-PHA	<i>Phaseolus vulgaris</i> Leucoagglutinin
E-PHA	<i>Phaseolus vulgaris</i> Erythroagglutinin
ConA	Concanavalin A
RT-PCR	Reverse transcription-polymerase chain reaction
PBS	10 mM phosphate-buffered saline (pH 7.4)
SDS	Sodium Dodecyl Sulfate
FITC	Fluorescein isothiocyanate
FCM	Flow Cytometry
CBB	Coomassie brilliant blue
HRP	Horse radish peroxidase

## Introduction

Complex N-glycans play very important roles in many different biological events, such as embryonic development, growth and cell differentiation. Biosynthesis of complex N-glycans are catalyzed by the action of *N*-acetylglucosaminyltransferases (GnTs) in the medial-Golgi apparatus, which add antennae branching structures on a common core structure of Man<sub>3</sub>GlcNAc<sub>2</sub>. The *Mgat4a*-encoded GnT-IVa glycosyltransferase is one of two isozymes that are primarily responsible for

J. Fan · S. Wang · S. Yu · J. He · W. Zheng · J. Zhang (✉)  
Department of Biochemistry, Institute of Glycobiology,  
Dalian Medical University,  
Dalian, 116044, China  
e-mail: jnzhang@dlmedu.edu.cn

the formation of the GlcNAc  $\beta$ 1-4 branch on the GlcNAc  $\beta$ 1-2Man  $\alpha$ 1-3 arm of the core structure on N-Glycans [1–3]. This distinct N-glycan branch catalyzed by GnT-IVa is the common substrate for GnT-III and GnT-V [4]. Therefore, GnT-IVa is one of the key glycosyltransferases regulating formation of tri- and other multiantennary structures (Fig. 1). It is well known that cancer invasion and metastasis is often accompanied by an aberrant oligosaccharide expression of glycoproteins in tumor cells. Many studies show that alterations in N-linked oligosaccharides of tumor cells are related to carcinogenesis, invasion and metastasis [5–8]. For example, GnT-V, which catalyzes the formation of  $\beta$ 1-6GlcNAc branching on N-Glycans, is closely associated with malignant transformations [9–12], while GnT-III prevents the metastatic spreading of cancer cells [6, 13–15], which catalyzes the bisecting structure in N-Glycans. Studies have shown that GnT-IVa was involved in many different diseases including type 2 diabetes [16, 17], choriocarcinoma [18] and pancreatic cancer [19]. However, the relationship between GnT-IVa expression and metastasis of hepatocarcinoma has been investigated in very few studies [20]. Our recent study indicates that the expression of GnT-IVa in Hca-F cells was much higher than that in Hepa1-6 cells, these two mouse hepatocarcinoma cell lines have high and no metastatic potential in lymph nodes, respectively. Here, we explore the possibility that expression levels of GnT-IVa affect the metastatic potential of mouse hepatoma cells.

CD147, also named Extracellular Matrix Metalloproteinase Inducer (EMMPRIN), is a plasma transmembrane glycoprotein widely expressed on many cell types, and its expression is relatively high in many tumor cells [21, 22]. Studies indicate that tumor cell CD147 leads to increased tumor growth and metastasis by stimulating the production of multiple matrix metalloproteinases (MMPs) [23, 24], which can degrade extracellular matrix. CD147 contains two extracellular Ig domains,

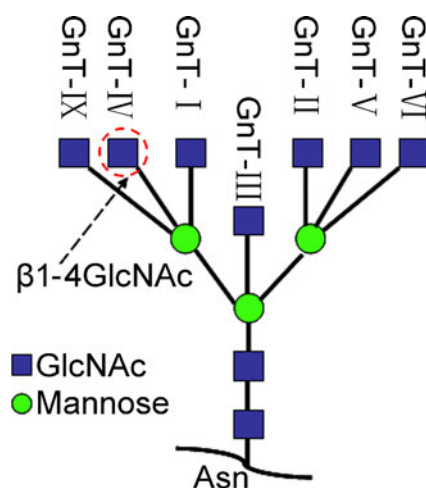


**Fig. 1** The antennary structure of N-glycan catalyzed by GnTs. GnT-IV produces  $\beta$ 1-4 branch on complex N-Glycan, while GnT-III and GnT-V catalyze the formation of bisecting and  $\beta$ 1-6 branches on N-Glycan respectively

which have three Asn glycosylation sites. Because of the heterogeneous N-glycosylation, CD147 shows both high glycosylated (HG)-CD147 (~40–60 kDa), and a low glycosylated (LG)-CD147 (~32 kDa) form. Wei Tang *et al.* reported that all CD147 glycosylation is N-linked, with HG-CD147 containing complex-type carbohydrates and LG-CD147 containing the high-mannose form [25].

In our previous study, CD147 was detected in mouse hepatocarcinoma Hca-F and Hepa1-6 cell lines. The results clearly indicated that HG-CD147 was mainly found in Hca-F cells, but weakly expressed in Hepa1-6 cells. On the contrary, LG-CD147 expression level was much higher in Hepa1-6 cells than in Hca-F cells [26]. Therefore, the HG-CD147 expression may contribute to lymphatic metastatic potential of mouse hepatocarcinoma cells. Quite interestingly, we found that GnT-IVa expression in Hepa1-6 cells is almost absent, but show high level in Hca-F. Taken together, high GnT-IVa expression is accompanied by a higher HG-CD147 form in Hca-F cells, which has high metastatic potential in lymph nodes, while low GnT-IVa expression comes with the LG-CD147 expression and shows no lymph nodes metastatic potential in Hepa1-6 cells. Thus, there should be a linkage between the GnT-IVa expression and the metastatic potential in mouse hepatoma cells.

In this study, the exogenous GnT-IVa was introduced in Hepa1-6 cells, which show very less GnT-IVa expression. On the other hand, the expression of GnT-IVa was down-regulated in Hca-F cells by lentivirus induced RNA interference. We undertook studies to identify the relationship between the function of GnT-IVa and lymphatic metastatic potential in mouse hepatoma cells and to determine whether the GnT-IVa expression affects the heterogeneously glycosylated forms of CD147.

## Materials and methods

### Cell culture

Mouse hepatocarcinoma Hca-F cell line (established and stored by Department of Pathology, Dalian Medical University) was cultured in 90 % RPMI-1640 (Gibco) supplemented with 1 % penicillin/streptomycin antibiotics (Gibco) and 10 % fetal bovine serum (Gibco) [27, 28]. Hepa1-6 cell line was obtained from cell bank of Chinese Academy Typical Culture Collection, and maintained in DMEM (Gibco) with 10 % fetal bovine serum (Gibco) containing 1 % penicillin/streptomycin. All cells were cultured in a humidified incubator at 37 °C with 5 % CO<sub>2</sub>.

### Quantitative RT-PCR assay

For the quantification of GnT-IVa in hepatoma cells, real-time RT-PCR was employed. Total RNAs were prepared using the RNAiso Reagent Plus (Takara). cDNAs were synthesized

using SYBR® PrimeScript™ RT-PCR kit (Takara). A standard curve for GnT-IVa was generated by the serial dilution using EASY dilution reagent (Takara). The primers were as follows: GnT-IVa-F 5'-CCACTGCGCTGGTATTTGTCAC-3', GnT-IVa-R 5'-CTATGCTCGGCCACTCGAAGA-3'; GAPDH-F 5'-AAATGGTGAAGGTCGGTGTG-3', GAPDH-R 5'-TGAAGGGGTCGTTGATGG-3'. Primers and cDNAs were added to Takara PCR thermal cycler dice real time system (Takara), which contained all reagents required for PCR.

#### Construction of overexpression vector

The whole coding region of *Mgat4a* was cloned into the pMD18-T Simple Vector (Takara) and then sub-cloned into a pcDNA3.1 expression vector (Invitrogen) resulting in pcDNA3.1/GnT-IVa. GnT-IVa cell line was constructed by transfecting the expression plasmid (pcDNA3.1/GnT-IVa) into Hepa1-6 cells. Empty vector pcDNA3.1 was also transfected as a mock. Stable GnT-IVa over-expression cell clones were selected with selection medium containing 800 µg/ml G418 and confirmed by GnT-IVa expression at mRNA and protein levels.

#### Construction of siRNA and retroviral infection

Short hairpin interfering oligonucleotides specific for GnT-IVa were designed on the openbiosystem website. The oligonucleotides were annealed and then ligated into pLL3.7 vector (Addgene). To obtain the lentivirus, two package plasmids were transfected into human embryonic kidney 293 T cells with constructed pLL3.7/GnT-IVa vector simultaneously using lipiofectamine2000 kit (Invitrogen) according to the manufacturer's protocol. Empty lentiviral vector acts as mock. The retroviral supernatant was collected 48 h after transfection. Mouse Hca-F cells were infected with the viral supernatant with 8 µg/ml polybrene (Sigma). Down-regulation of GnT-IVa in Hca-F cells was confirmed and named GnT-IVa i.

#### Semi-quantitative RT-PCR analysis

Total RNA was prepared from cells using TRIzol reagent (Invitrogen). 5 µg of total RNA was reverse transcribed into cDNA using AMV with oligo (dT) as a primer. Amplified cDNA by *r*Tag DNA polymerase (Takara) in PCR reaction using the following specific primer sets: GnT-IVa-F: 5'-CAGCTAGCATGAGGCTCCGAAATGGAAC-3' and GnT-IVa-R 5'-GAGGTACCCACTGGTGACTTTAATATG-3'; GAPDH-F: 5'-ATCTCTGCCCCCTCTGCTGA-3', and GAPDH-R: 5'-GATGACCTTGCCCACAGCCT-3'. The PCR products were electrophoresed in 1 % agarose gel. Band intensities were measured using Bioimaging systems (UVP, labworks™).

#### Western blot assay

Cells were washed with phosphate-buffered saline (PBS) twice and lysed with ice-cold lysis buffer (10 mM Tris-HCl (pH 7.8), 1 % NP-40, 0.15 M NaCl, 1 mM EDTA and a mixture of protease inhibitors). The cell lysates were centrifuged at 14,000 g for 15 min at 4 °C. The supernatant was collected and protein concentration was determined by BCA kit (Pierce). Equal amount of proteins were separated by 10 % or 8 % SDS-PAGE, respectively. Then, proteins were transferred to nitrocellulose membrane. The membrane was blocked in Tris-buffered saline (TBS) with 5 % nonfat milk for 1 h at room temperature, followed by incubation with appropriate primary antibodies at 4 °C overnight. After washing in TBS-Tween 20 buffer, membranes were incubated for 2 h with the appropriate peroxidase-conjugated secondary antibodies. After washing in TBS-Tween 20 buffer, the protein bands on the membranes were visualized using ECL kit (GE healthcare).

#### Lectin blot analysis

Cells were harvested and lysed, proteins extracted from the cells were electrophoresed on 8 % SDS-PAGE and protein-blotted nitrocellulose membranes were prepared in exactly the same way as described for western blot. After blocking with Carbo-Free Blocking Solution (Vector labs), the membrane was incubated with 2 µg/ml various biotinylated lectins (Vector labs) for 30 min. Reactive bands were detected with a diluted horseradish peroxidase (HRP) conjugated streptavidin (Vector labs), and then visualized using ECL system (GE Healthcare).

#### Immunoprecipitation

Cells in 10-cm dishes were collected and lysed in RIPA buffer (50 mM Tris (pH 7.4), 1 % NP-40, 0.15 M NaCl, 1 % Triton X-100, 1 mM EDTA, 1 % sodium deoxycholate, 0.1 % SDS and a mixture of protease inhibitors). Mouse polyclonal antibody against CD147 (Santa Cruz) was incubated with the cell lysis at 4 °C overnight in lysis buffer. The immunoprecipitates were washed twice with cold lysis buffer, followed by incubation with Sepharose Protein A (GE Healthcare), which had been prewashed with PBS containing 1 % BSA. Finally, the beads were washed, boiled, centrifuged and the recovered samples were run on 8 % SDS-PAGE for lectin blot as described above.

#### Transwell migration assay

To evaluate cell migration capability, transwell plates (Corning Incorporated) with a filter of 6.5 mm diameter and 8.0 µm pore size were used [29]. Transwell chambers were

inserted into 24-well plate.  $1 \times 10^5$  cells were plated in the upper compartment in 200  $\mu$ l serum free medium per chamber, and 500  $\mu$ l of complete medium was added to the lower wells. The chambers were incubated for 24 h at 37 °C in 5 % CO<sub>2</sub> to allow cells to migrate from the upper chamber to the lower well. Cells migrating through the pores and adherent on the undersurface of the membrane were stained with crystal violet. The number of cells was counted under a microscope at  $\times 200$  magnification. Data were obtained from three individual experiments performed in triplicate.

#### Flow cytometry (FCM) analysis

Cells were treated with trypsin and centrifuged at 800 rpm for 5 min. Cell pellets were suspended in 100  $\mu$ l PBS with Triton X-100 for 5 min, then, FITC-labeled lectins, including L-PHA and E-PHA, were added to a final concentration of 2  $\mu$ g/ml and incubated at room temperature for 30 min. For the detection of GnT-IVa expression, first the primary anti GnT-IVa antibody was added to the cell lysis, washed with PBS followed by TRITC-labeled secondary antibody. After rinsed twice with cold PBS, fluorescent analysis was performed using a FACScalibur (Becton Dickinson). Only live cells were established as gates, unstained cells served as controls.

#### Wound-healing assay

Wound healing assay was performed as previously reported [30, 31]. Briefly, cells were plated in a 12-well plate and incubated overnight yielding confluent monolayers. Wounds were made using a pipette tip and photographs taken immediately (time zero) and 16 h after wounding. The area migrated by the cell monolayer to close the injury line was measured. Experiments were carried out in the three neighboring wells and repeated at least three times.

#### Soft-agar colony-formation assay

To determine the transformation potential of the cells, colony-formation assay was performed in 6-cm dishes (in triplicate). The bottom layer of medium containing 10 % fetal bovine serum, 1 % penicillin and streptomycin with agar (low melt 0.7 %) was poured first, after solidifying, this is followed by a top layer containing the same medium with 1.2 % agar, mixed with 1,000 cells. The plates were placed in a humidified incubator at 37 °C with 5 % CO<sub>2</sub> for 2 weeks. The plates were photographed and the numbers of distinct colonies ( $\geq 50$  cells per colony) were counted under a light microscope. The results averaged for each treatment group.

#### *In vivo* animal experiments

$1 \times 10^6$  cells of GnT-IVa transfectant and wild type were injected subcutaneously into the right flanks of C57L/J mice. After 2 weeks, the mice were sacrificed. The tumors were isolated, weighed, sectioned, and stained with hematoxylin and eosin. The GnT-IVa and CD147 expression were detected by immunohistochemistry and lectin histochemistry

Hematoxylin and eosin (HE) staining,  
immunohistochemistry and lectin histochemistry

Tumor specimens were fixed in 10 % formalin and embedded in paraffin. Paraffin specimens were cut at a thickness of 4  $\mu$ m. For HE Staining, paraffin-embedded sections were deparaffinized in xylene and rehydrated through graduate ethanol to water, after staining with Mayer's hematoxylin for 15 min, the slides were washed in running tap water for 20 min. Counterstaining with eosin for about 30 s followed by dehydration in 95 % and 100 % alcohol, sections were observed under light microscope after clear in xylene.

Immunohistochemical staining was performed using the streptavidin-peroxidase conjugated method (SP method). Endogenous peroxidase activity was blocked by incubation with 0.3 % H<sub>2</sub>O<sub>2</sub>, and nonspecific immunoglobulin binding was blocked by incubation with 10 % normal goat serum. Sections were incubated at 4 °C overnight with diluted primary antibody. The sections were rinsed and incubated with the biotinylated secondary antibody. After washing, the sections were incubated with HRP conjugated streptavidin, and finally treated with 3'3-diaminobenzidine tetrahydrochloride. The sections were stained by 3'3-diaminobenzidine (DAB) to visualize antigen-antibody complex. The nuclei were then counterstained with Mayer's hematoxylin.

The expression of branching asparagine-linked oligosaccharides was analyzed by lectin histochemistry described in a previous study [32]. The procedures were almost the same with immunohistochemistry. Briefly, without incubation with biotinylated secondary antibody, the biotinylated lectin including L-PHA and E-PHA react with HRP conjugated streptavidin directly. Final staining was performed also with DAB. All the slides were observed under microscope and photographed.

#### Statistical analysis

Statistical analyses were performed using SPSS 13.0 software. Each assay was performed at least three times. Data were expressed as mean  $\pm$  S.D. Student's *t*-test was used to evaluate the significance of data. *P* values  $< 0.05$  were considered as statistically significant.

## Results

### GnT-IVa expression in hepatoma cells

*Mgat4a* encoded gene expression of GnT-IVa was detected in different lymphatic potential hepatocarcinoma cell lines Hepa1-6 and Hca-F. The expression of GnT-IVa was much higher in Hca-F cells than that in Hepa1-6 cells (Fig. 2). Thus, the expression of GnT-IVa tends to be related to the lymphatic potential in hepatoma cells.

### Overexpression of GnT-IVa in Hepa1-6 cells

The whole CDS region of *Mgat4a* gene was cloned into the pcDNA3.1 expression vector and then resulting in Hepa1-6/GnT-IVa cells. The empty pcDNA3.1 vector was transfected into Hepa1-6 cells as Mock. RT-PCR (Fig. 3a) and western blot (Fig. 3b) analyses showed the stable over-expression of GnT-IVa in Hepa1-6 cell line.

### Down regulation of GnT-IVa in Hca-F cells

After retroviral infection, infected Hca-F cells were harvested and the expression of GnT-IVa was measured by RT-PCR. This data showed the GnT-IVa was down-regulated by 80 % compared with those in wild type and mock cells (Fig. 4a). FCM analysis also showed significantly silenced GnT-IVa expression in Hca-F cells (GnT-IVa i) after the retroviral infection (Fig. 4b).

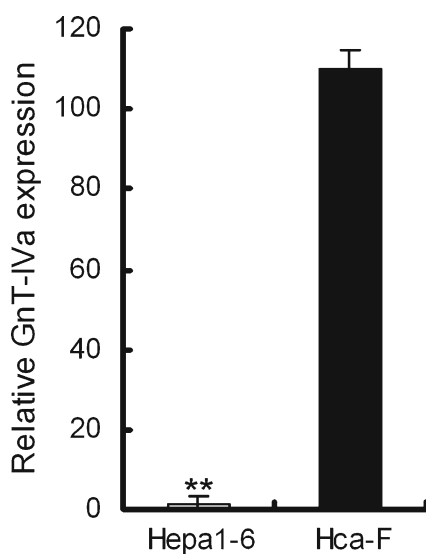


**Fig. 2** Quantitative RT-PCR analysis of GnT-IVa transcript in Hca-F and Hepa1-6 cells. The relative amount of GnT-IVa transcript was normalized to the amount of GAPDH transcript. Data were obtained from triplicate experiments and are indicated as means  $\pm$  S.D.  $**P < 0.01$

### Alteration of oligosaccharide structures affected by GnT-IVa expression

Glycosylation of glycoproteins with *N*-acetylglucosamine (GlcNAc) is a dynamic protein modification [33]. The separated glycoproteins were transferred onto nitrogen membrane and then stained using HRP-L-PHA and HRP-E-PHA. These results revealed that the antennary branches on glycoproteins were altered by different GnT-IVa expression level. The intensity of HRP-L-PHA staining in Hepa1-6/GnT-IVa cells was significantly increased, while E-PHA signal decreased (Fig. 5a). FCM assay show the consistent alteration of oligosaccharide structures with lectin blot analysis (Fig. 5b). On the contrary, HRP-L-PHA staining decreased with silenced GnT-IVa expression in Hca-F cells (GnT-IVa i), but no significant change of HRP-E-PHA signal (Fig. 5c). These data indicated that the oligosaccharide structures of N-glycans in glycoproteins were altered generally, due to the expression of GnT-IVa in mouse hepatoma cells.

### The effects of GnT-IVa on metastatic capability *in vitro*

We assessed the effect of GnT-IVa on tumor metastatic capability by transwell assay system. As shown, GnT-IVa overexpression in Hepa1-6 cells has a greater potential to migrate than wild type and mock cells. In contrast, migration of Hca-F cells with silenced GnT-IVa expression was impeded compared to that of wild type and mock (Fig. 6a and b). Likewise, in wound-healing assay, within 16 h after scratching, the Hepa1-6/GnT-IVa-seeded plates were more completely healed than those of wild type and mock cells (Fig. 6c and d). Soft-agar colony-formation assay *in vitro* further confirm the effect of GnT-IVa on tumor metastatic capability. As shown that the colony numbers and size of GnT-IVa i cells were apparently less and smaller than those of Hca-F and mock cells. While more and larger colonies formed in GnT-IVa overexpressed group (Fig. 6e and f). Taken together, the data suggest that the expression of GnT-IVa markedly affects cell migration and tumorigenicity.

### Effect of GnT-IVa on glycosylation of CD147

Western blot analysis revealed that almost no HG-CD147 expression in Hepa1-6 cells and mock group, but greater amounts of HG forms of CD147 were observed in GnT-IVa stable over-expressed cells, while in Hca-F, Mock and GnT-IVa i cells, HG-CD147 expression reduced apparently with silenced GnT-IVa expression compared to wild type and mock (Fig. 7a). Furthermore, after the immunoprecipitation with anti-CD147 antibody, variability of antennary branches in the CD147 N-glycosylation was detected by lectin blot with L-PHA and E-PHA staining.

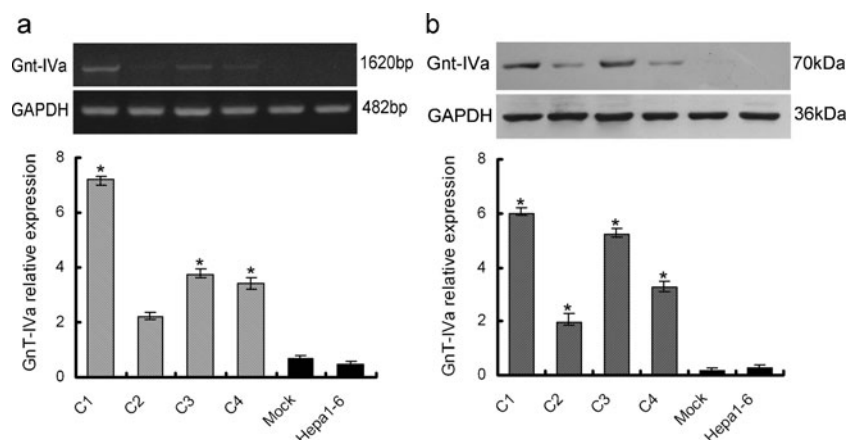


**Fig. 3** Identification of the GnT-IVa overexpression in Hep1-6 cells. Hep1-6 cells were stably transfected with the pcDNA3.1/GnT-IVa and empty plasmids. GnT-IVa mRNA and protein content were analyzed by RT-PCR and western blot assay respectively. Mock, empty vector

transfectants; C1 to C4 represents transfected pcDNA3.1/GnT-IVa stable cell clones. GAPDH was used as control. **a** Overexpressed GnT-IVa was identified by RT-PCR. **b** Detection of GnT-IVa protein expression by western blot. \* $p < 0.05$

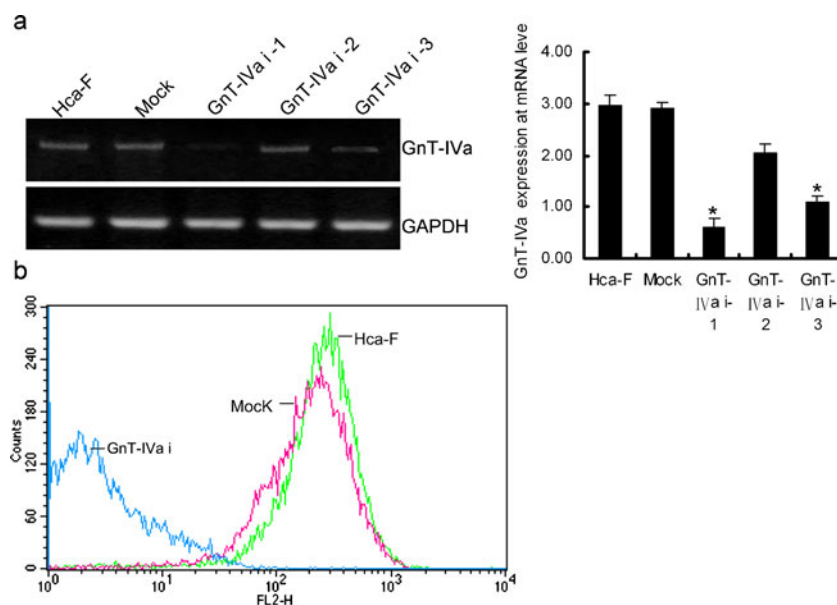
The data showed that there are increased  $\beta$ 1-6GlcNAc branches and decreased bisecting branches on CD147 in overexpressed GnT-IVa cell line, down-regulation of GnT-IVa in Hca-F cells results in decreased  $\beta$ 1-6GlcNAc branching but bisecting branching remains the same on CD147 (Fig. 7b). Lectin blot assay from total cell lysate protein revealed the similar results (Fig. 5a and c). Therefore, the variation of antennary branches on CD147 indicated that CD147 would be a target glycoprotein affected by GnT-IVa.

#### GnT-IVa regulates N-glycans *in vivo*

Tumors were isolated from mice after the injection of cells in right flanks. The tumor tissues are apparently larger in the GnT-IVa group than that in wild type Hep1-6 (Fig. 8a). Higher expression of GnT-IVa was detected by immunohistochemistry

in tumor sections, whereas the wild type group showed weak GnT-IVa immunostaining (Fig. 8b). Next, we examined the expression of branching oligosaccharides by lectin histochemistry in the same sections, simultaneously. Tumor cells with higher GnT-IVa expression showed strong L-PHA staining and very weak E-PHA. In contrast, the L-PHA signal was weak and the E-PHA staining strong in wild type tumors (Fig. 8c), even though there was no significant change of CD147 (Fig. 8b). These results were consistent with those of lectin blot analysis *in vitro* (Fig. 5a).

**Fig. 4** Downregulation of GnT-IVa in Hca-F cells. **a** The relative expression of GnT-IVa was measured by RT-PCR. The data show the silencing GnT-IVa expression in Hca-F cells. GnT-IVa i-1, 2, 3 represent infected Hca-F groups with different lentivirus/siRNA sequences. **b** FCM analysis also show significantly silenced GnT-IVa expression in Hca-F cells. TRITC-labeled secondary antibody was used to detect the fluorescence signal. \* $P < 0.05$



#### Discussion

N-acetylglucosaminyltransferase (GnT) -IV is one of the members of GnT family, which catalyze the formation of

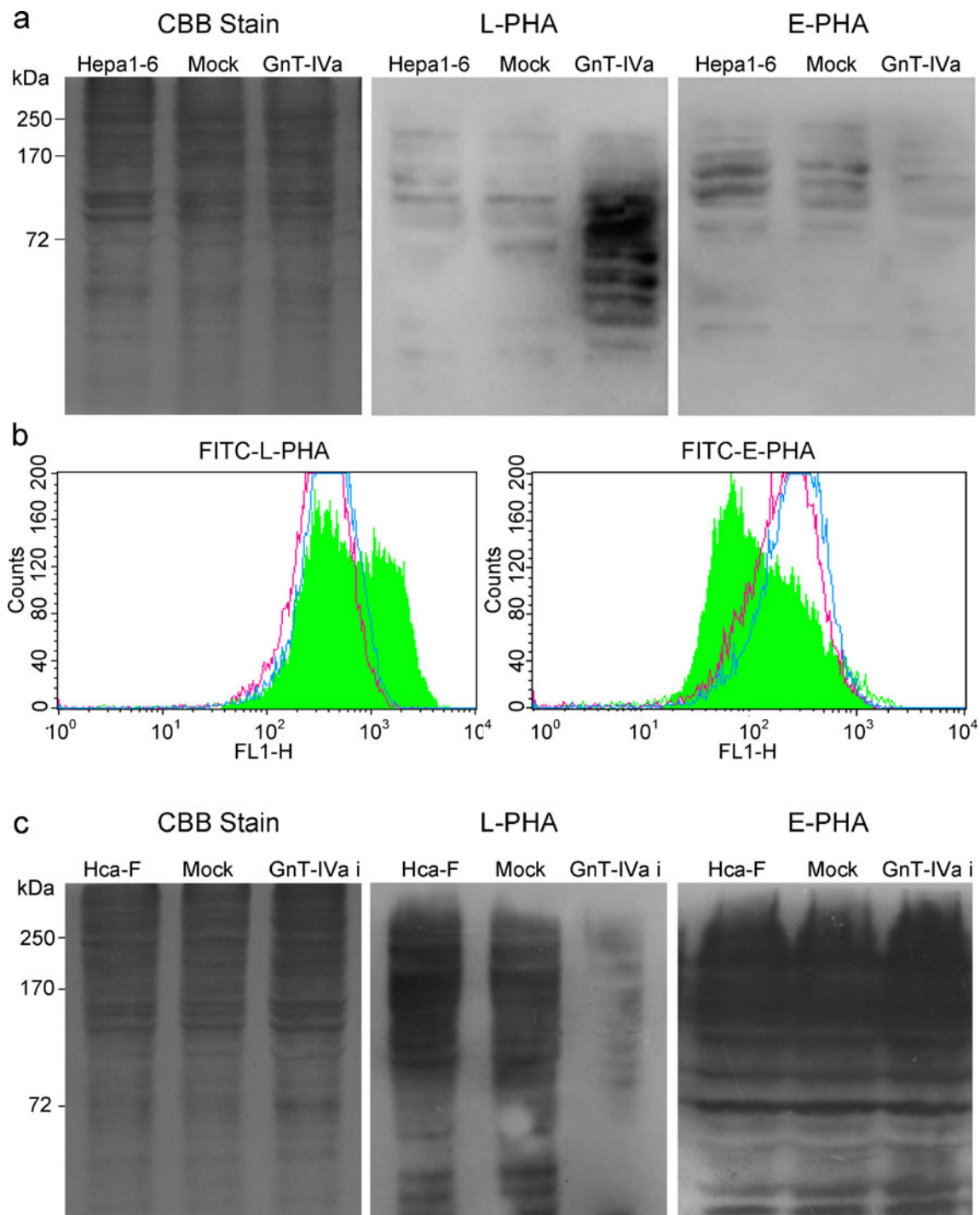


**Fig. 5** Analyses of oligosaccharide structures by lectin blot and FCM assay. **a** In Hepa1-6, Mock and GnT-IVa overexpressed hepa1-6 cells (GnT-IVa), the oligosaccharide structures were detected by lectin blot assay with HRP labeled L-PHA and E-PHA lectin. Mock, Hepa1-6 cells transfected with pcDNA3.1 vector. **b** FITC-labeled L-PHA and E-PHA lectin were measured by FCM analysis (pink and blue line represents

Hepa1-6 cells and Mock cells respectively. Green area means the altered FITC signal in GnT-IVa group). FCM assay show the consistent alteration of oligosaccharide structures with lectin blot analysis. **c** Lectin blot assay was performed in Hca-F cells. Mock, empty letivirus infected Hca-F cells; CBB stain as control

branching structures in complex N-glycans in the Golgi apparatus. At least, six different types of GnTs (GnT-I to VI) have been cloned and characterized [2, 34–37]. GnT-IV catalyzes

the transfer of GlcNAc from UDP-GlcNAc to Man $\alpha$ 1-3 arm of the common core structure, thus result in a  $\beta$ 1-4 branch. The regulation of GnT-IV expression has been investigated

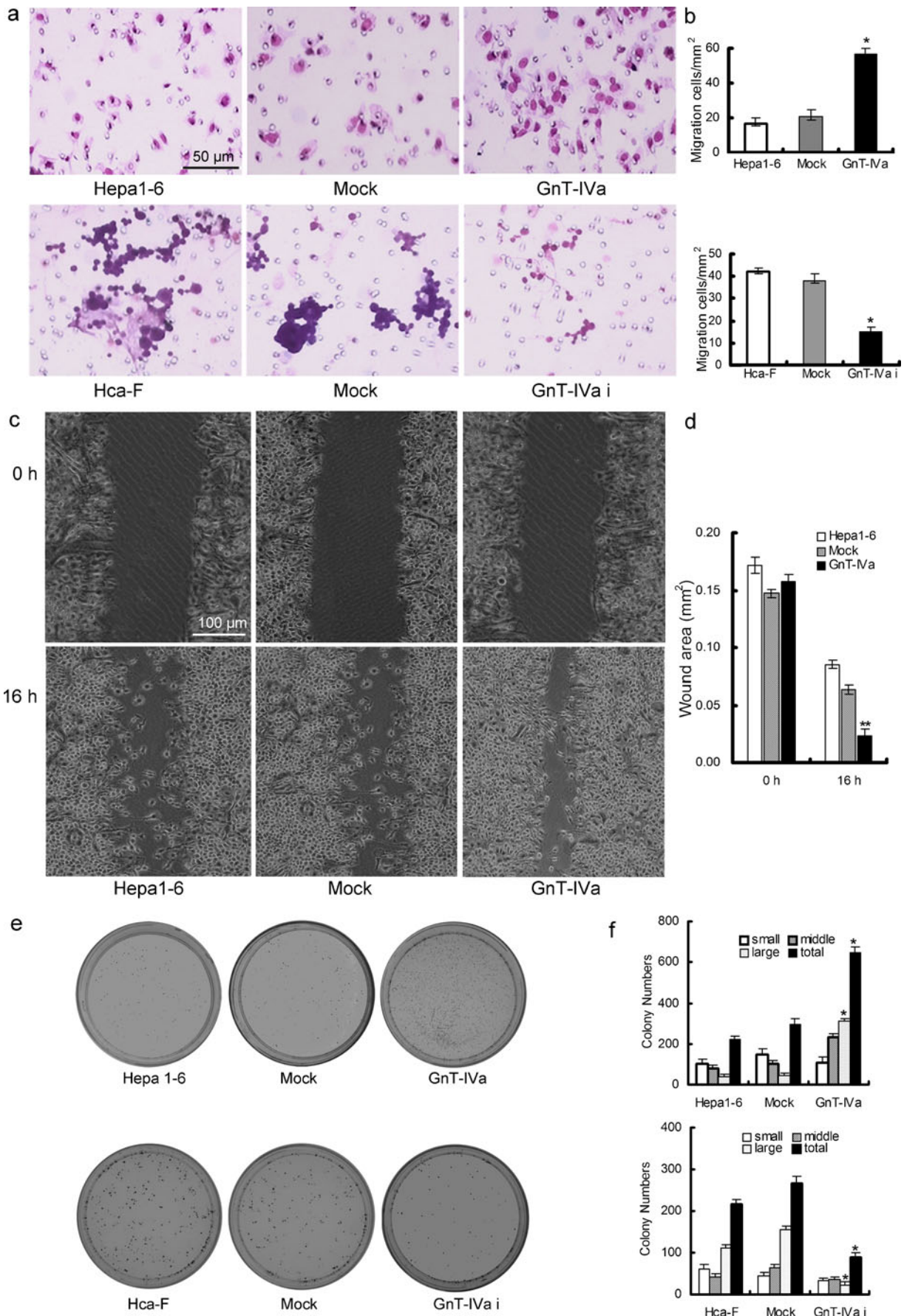




**Fig. 6** Cell metastatic capability detection. **a** Cells were seeded into a transwell chamber. The cells that migrated through membrane were fixed and stained with 0.1 % crystal violet and then examined under a light microscope. Representative examples were photographed at 200 x magnification. **b** The number of migrating cells was determined by counting the stained cells. Mock, transfected Hepa1-6 cells with empty vector and Hca-F cells infected with empty lentivirus. **c** In Hepa1-6, Mock and GnT-IVa cells, an injury line was made on a confluent monolayer of cells. Cell motility was examined with a light microscope (40 x) at the indicated time points (0 and 16 h). **d** The wounding area was quantified. **e** Colony-formation assay was performed in 6 cm dishes, each plate contain 4,000 indicated cells. After incubation at 37 °C in 5 % CO<sub>2</sub>, cells colonies were photographed. **f** Colonies were counted under the microscope according to diameter (small, less than 0.3 mm; middle, 0.3 mm~0.6 mm; large, more than 0.6 mm). Data expressed as the mean ± S.D. from 3 independent experiments. \**P*<0.05

during oncogenesis and differentiation. The aberrant antennary sugar chains with GlcNAc  $\beta$ 1-4 Man $\alpha$ 1-3 branch appeared in human chorionic gonadotropin (hCG) from choriocarcinoma patients, and the increased GnT-IV activity has been found in choriocarcinoma [38, 39]. Upregulated GnT-IV activity has also been reported in human hepatoma tissue [40]. Two isoenzymes of GnT-IV (GnT-IVa and GnT-IVb) have

been identified and study showed that GnT-IVa is more active than GnT-IVb. Therefore, it is GnT-IVa that primarily contributes to the biosynthesis of  $\beta$ 1-4 branch of N-glycans, although northern blot analysis revealed that GnT-IVb is more expressed in tissues than GnT-IVa [3]. On the other hand, the relationship between the numbers of antennae in complex N-glycans of mammalian cells and the expression of GnTs has been extensively observed. Especially, studies on GnT-III and GnT-V show the contrast functions. It has been reported that GnT-V expression levels involved in cell-matrix adhesion, cell migration and invasion, furthermore, enhance the carcinogenesis and tumor metastatic potential [41–44]. While, GnT-III might play a very important role in antagonizing the function of GnT-V because of the formation of bisecting oligosaccharide structure in complex N-glycans [14, 45]. However, the roles of GnT-IVa in tumor metastatic potential have been studied in very few works. Thus, we focus our study on the regulation of GnT-IVa expression during oncogenesis and metastasis in mouse hepatocarcinoma cells.

We choose the Hepa1-6 and Hca-F cell lines because of their different metastatic and invasive properties. Hca-F cells have highly invasive and metastatic potential in lymph nodes, while, Hepa1-6 cells do not. Northern blot analysis showed higher GnT-IV expression in lymphoid tissues such as spleen, thymus, lymph node, and peripheral blood leukocytes [46]. Interestingly, our present investigation demonstrated that Hca-F cells express very high GnT-IVa compared to that in Hepa1-6 cells (Fig. 2). Therefore, these two mouse hepatocarcinoma cell lines would be well as a model to detect whether the expression of GnT-IVa correlates with aberrant N-glycans associated with the development of metastasis in hepatocarcinoma. In this study, after stable transfection of Hepa1-6 cells with exogenous GnT-IVa cDNA, dramatic improvement on migration and transformation potential has been found both *in vitro* and *in vivo*. On the other hand, the results show that the inhibition of migration was associated with down-regulated GnT-IVa expression in Hca-F cells.

Whether the above biological effects are due to the alteration of antennary oligosaccharide branches in complex N-glycans is a question? The product formed by GnT-IVa catalysis serves as the common substrate for other GnTs, such as GnT-III and -V. Our results indicated that overexpression of GnT-IVa leads to the increase of  $\beta$ 1-6 sugar branches and the decrease of bisecting structure in Hepa1-6 cells. By contrast, decreased  $\beta$ 1-6 oligosaccharide structure is observed in GnT-IVa silenced Hca-F cells when compared to the wild type and mock cells. However, there is no effect of down-regulated GnT-IVa on bisecting sugar in Hca-F cells. These findings suggest that GnT-IVa may have a key role in the formation of the complicated antennary structures in complex N-glycans *via* interaction with other GnTs. GnT-IV gene is located on chromosome 2, band q12. Data shows that the human GnT-V gene (2q21) is located in close proximity to GnT-IV [35],

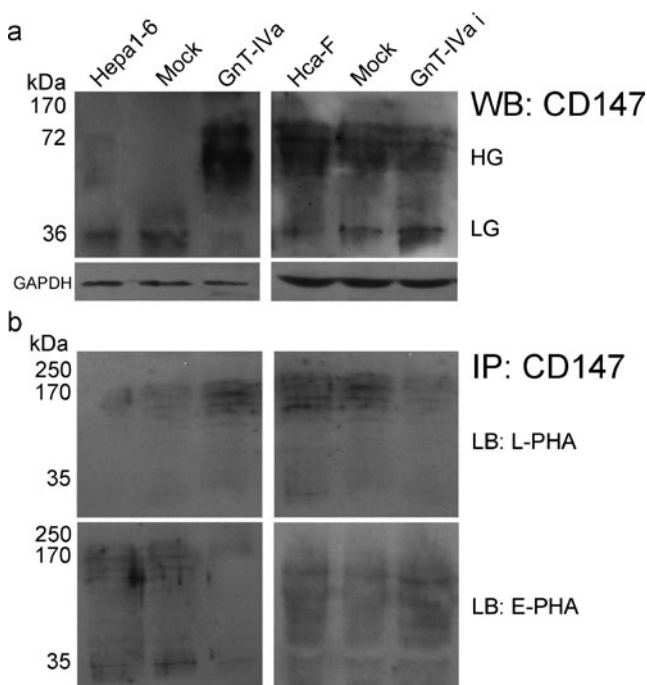


**Fig. 7** Western blot and immunoprecipitation plus lectin blot were performed. **a** Western blot show that GnT-IVa converts LG and HG-CD 147 from in hep1-6 and Hca-F cells, while the downregulated GnT-IVa in Hca-F cells leads to the decrease of HG-CD147. **b** After immunoprecipitation using antiCD-147 antibody-protein A beads complex, lectin blot results show the increased  $\beta$ 1-6 antennary oligosaccharide sugar chains and the decreased bisecting branch on the CD147. On the contrary, weak L-PHA staining signal represents decreased  $\beta$ 1-6 antennary oligosaccharide sugar chains on the CD-147 with downregulated GnT-IVa in Hca-F cells, but no change of E-PHA staining signal

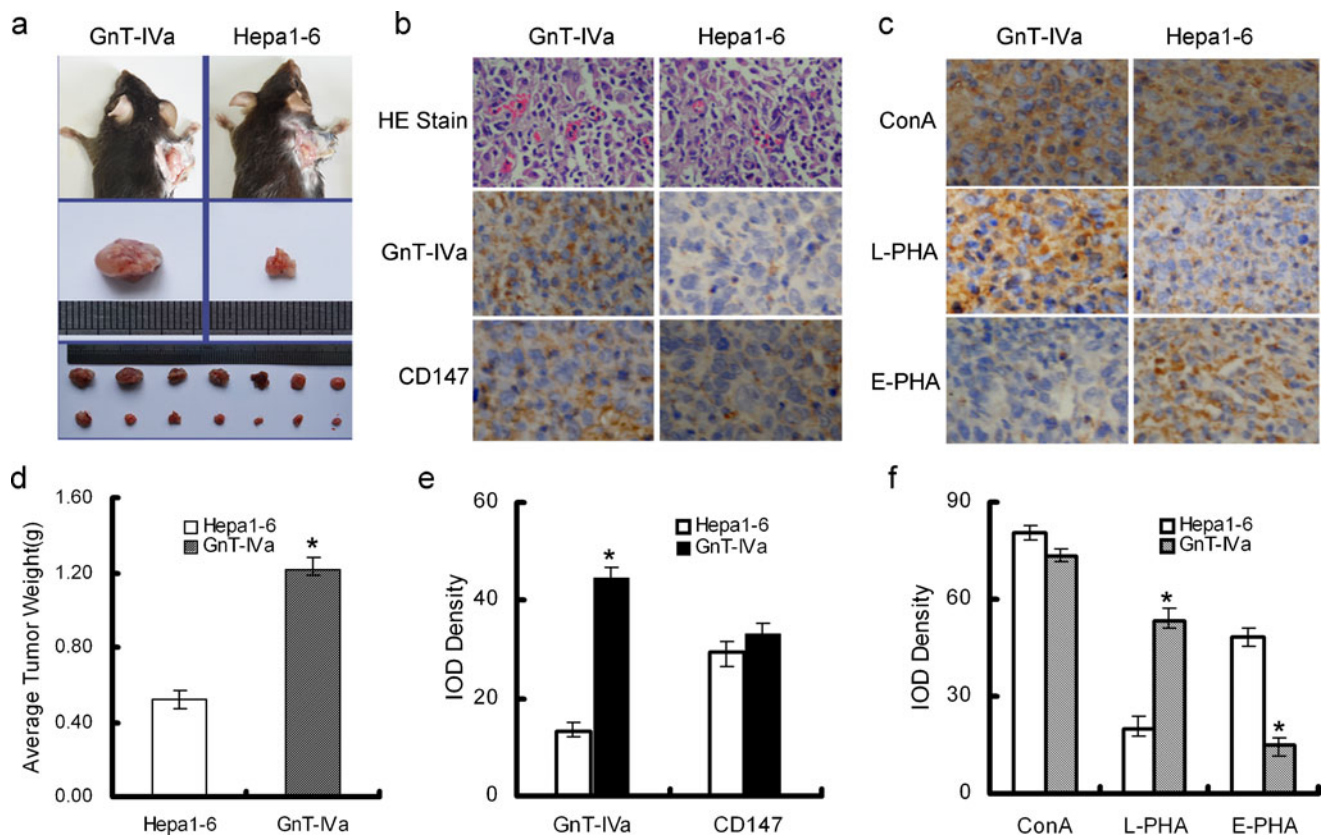


**Fig. 8** The wide type and GnT-IVa overexpressed Hepa1-6 cells were injected in the back of C57L/J mouse. After 2 weeks, mice are sacrificed and tumors were isolated from mice, photographed and treated. **a** Sacrificed mouse and the isolated tumor were measured by size and weight. **b** 4  $\mu\text{m}$ -thick tumor sections were stained with routinely HE staining (upper panel), less microvessels in wide type group (upper panel). Anti GnT-IVa antibody and anti CD147 antibody was detected by immunohistochemistry respectively. **c** Lectin histochemistry was

performed with ConA, E-PHA and L-PHA lectin. The result show that increased GnT-IVa expression was found in Hepa1-6/GnT-IVa mouse tumor with increased L-PHA staining and decreased E-PHA staining. **d-f** SP method was used to detect the signal and IOD density was measured using *image pro plus* system. Representative photos were taken under Olympus lighter microscope at 400 x magnification. Bars represent the mean  $\pm$  S.D. \* $P < 0.05$

and the human GnT-IV gene has multiple exons similar to GnT-III [47] and -V [48]. The amino acid sequence identity between human and mouse is 94 %, such a high conservation of GnT-IV amino acid sequence suggests that a highly restricted protein structure is required for recognizing an 1, 3 monoxide and several GlcNAc branches of acceptor complex N-glycans [49]. It is noteworthy in our study that the engineered overexpression of GnT-IVa in Hepa1-6 cells affected the expression of GnT-III and -V significantly (data not shown). The sequence for translational initiation of human GnT-IV does not fully satisfy the Kozak consensus sequence [50]. All these features may suggest that, for these three GnTs, there should be a correct order in catalyzing the formation of antennary branches in complex N-glycans, or perhaps, they share the same transcription factors which regulate the gene expression during the transcription initiation process. All these aspects will require further study.

Our previous study showed that CD147 correlates with HG form contribute to lymphatic metastasis potential in mouse hepatocarcinoma cells [51]. The data clearly indicated that

CD147 was strongly expressed on Hca-F cells with lymphatic metastatic potential but less on Hepa1-6 cells without lymphatic metastatic potential. Significantly, greater amounts of HG-CD147 were observed, relative to the LG forms in Hca-F cells. However, the HG-CD147 was relatively scarce while the LG form CD147 was common in Hepa1-6 cells. Furthermore, immunoprecipitation and L-PHA lectin blot analyses showed that  $\beta$ 1-6 branches were observed on CD147 in Hca-F cells but very weak L-PHA signal been detected on CD147 in Hepa1-6 cells (data not show). In this study, exogenous GnT-IVa caused dramatic alteration of the glycosylated forms on CD147 and enhanced the L-PHA signal on CD147.

In conclusion, the exogenous expression of in GnT-IVa in Hepa1-6 cells increased their antennary oligosaccharide structure and exhibited enhanced migration and transformation potential both *in vitro* and *in vivo*. In addition, CD147 in Hepa1-6 cells converse from LG to HG-CD147 form. In contrast, down-regulation of GnT-IVa in Hca-F cells showed reduced antennary branches of N-Glycans, and significantly decreased the migration and metastatic capability *in vitro*. Our

results suggest that expression of GnT-IVa may affect the metastatic potential of mouse hepatoma cells through glycosylation of CD147.

**Acknowledgements** This work was supported by grants from the National Program on Key Basic Research Project (973 Program) (NO. 2012CB822103) and National Science Fund Committee (NSFC) (NO. 30970648, 31000372, 31170774)

## References

- Minowa, M.T., Oguri, S., Yoshida, A., Hara, T., Iwamatsu, A., Ikenaga, H., Takeuchi, M.: cDNA cloning and expression of bovine UDP-N-acetylglucosamine: alpha1, 3-D-mannoside beta1,4-N-acetylglucosaminyltransferase IV. *J. Biol. Chem.* **273**(19), 11556–11562 (1998)
- Yoshida, A., Minowa, M.T., Takamatsu, S., Hara, T., Ikenaga, H., Takeuchi, M.: A novel second isoenzyme of the human UDP-N-acetylglucosamine:alpha1,3-D-mannoside beta1,4-N-acetylglucosaminyltransferase family: cDNA cloning, expression, and chromosomal assignment. *Glycoconj. J.* **15**(12), 1115–1123 (1998)
- Oguri, S., Yoshida, A., Minowa, M.T., Takeuchi, M.: Kinetic properties and substrate specificities of two recombinant human N-acetylglucosaminyltransferase-IV isozymes. *Glycoconj. J.* **23**(7–8), 473–480 (2006). doi:10.1007/s10719-006-6216-3
- Schachter, H., Brockhausen, I., Hull, E.: High-performance liquid chromatography assays for N-acetylglucosaminyltransferases involved in N- and O-glycan synthesis. *Methods Enzymol.* **179**, 351–397 (1989)
- Taniguchi, N., Korekane, H.: Branched N-glycans and their implications for cell adhesion, signaling and clinical applications for cancer biomarkers and in therapeutics. *BMB Rep.* **44**(12), 772–781 (2011)
- Isaji, T., Kariya, Y., Xu, Q., Fukuda, T., Taniguchi, N., Gu, J.: Functional roles of the bisecting GlcNAc in integrin-mediated cell adhesion. *Methods Enzymol.* **480**, 445–459 (2010). doi:10.1016/S0076-6879(10)80019-9
- Saldova, R., Reuben, J.M., Abd Hamid, U.M., Rudd, P.M., Cristofanilli, M.: Levels of specific serum N-glycans identify breast cancer patients with higher circulating tumor cell counts. *Ann. Oncol.* **22**(5), 1113–1119 (2010). doi:10.1093/annonc/mdq570
- Bones, J., Mittermayr, S., O'Donoghue, N., Guttman, A., Rudd, P.M.: Ultra performance liquid chromatographic profiling of serum N-glycans for fast and efficient identification of cancer associated alterations in glycosylation. *Anal. Chem.* **82**(24), 10208–10215 (2010). doi:10.1021/ac102860w
- Tsui, K.H., Chang, P.L., Feng, T.H., Chung, L.C., Sung, H.C., Juang, H.H.: Evaluating the function of matriptase and N-acetylglucosaminyltransferase V in prostate cancer metastasis. *Anticancer Res.* **28**(4A), 1993–1999 (2008)
- Chakraborty, A.K., Pawelek, J., Ikeda, Y., Miyoshi, E., Kolesnikova, N., Funasaka, Y., Ichihashi, M., Taniguchi, N.: Fusion hybrids with macrophage and melanoma cells up-regulate N-acetylglucosaminyltransferase V, beta1-6 branching, and metastasis. *Cell Growth Differ.* **12**(12), 623–630 (2001)
- Guo, H.B., Liu, F., Zhao, J.H., Chen, H.L.: Down-regulation of N-acetylglucosaminyltransferase V by tumorigenesis- or metastasis-suppressor gene and its relation to metastatic potential of human hepatocarcinoma cells. *J. Cell. Biochem.* **79**(3), 370–385 (2000). doi:10.1002/1097-4644(20001201)79:3<370
- Murata, K., Miyoshi, E., Kameyama, M., Ishikawa, O., Kabuto, T., Sasaki, Y., Hiratsuka, M., Ohigashi, H., Ishiguro, S., Ito, S., Honda, H., Takemura, F., Taniguchi, N., Imaoka, S.: Expression of N-acetylglucosaminyltransferase V in colorectal cancer correlates with metastasis and poor prognosis. *Clin. Cancer Res.* **6**(5), 1772–1777 (2000)
- Yoshimura, M., Nishikawa, A., Ihara, Y., Taniguchi, S., Taniguchi, N.: Suppression of lung metastasis of B16 mouse melanoma by N-acetylglucosaminyltransferase III gene transfection. *Proc. Natl. Acad. Sci. U.S.A.* **92**(19), 8754–8758 (1995)
- Zhao, Y., Nakagawa, T., Itoh, S., Inamori, K., Isaji, T., Kariya, Y., Kondo, A., Miyoshi, E., Miyazaki, K., Kawasaki, N., Taniguchi, N., Gu, J.: N-acetylglucosaminyltransferase III antagonizes the effect of N-acetylglucosaminyltransferase V on alpha3beta1 integrin-mediated cell migration. *J. Biol. Chem.* **281**(43), 32122–32130 (2006). doi:10.1074/jbc.M607274200
- Zhao, Y., Sato, Y., Isaji, T., Fukuda, T., Matsumoto, A., Miyoshi, E., Gu, J., Taniguchi, N.: Branched N-glycans regulate the biological functions of integrins and cadherins. *FEBS J.* **275**(9), 1939–1948 (2008). doi:10.1111/j.1742-4658.2008.06346.x
- Ohtsubo, K., Takamatsu, S., Minowa, M.T., Yoshida, A., Takeuchi, M., Marth, J.D.: Dietary and Genetic Control of Glucose Transporter 2 Glycosylation Promotes Insulin Secretion in Suppressing Diabetes. *Cell*, (2005)
- Ohtsubo, K., Chen, M.Z., Olefsky, J.M., Marth, J.D.: Pathway to diabetes through attenuation of pancreatic beta cell glycosylation and glucose transport. *Nat. Med.*, online (2011)
- Takamatsu, S., Oguri, S., Minowa, M.T., Yoshida, A., Nakamura, K., Takeuchi, M., Kobata, A.: Unusually high expression of N-Acetylglucosaminyltransferase-IVa in human choriocarcinoma cell lines: a possible enzymatic basis of the formation of abnormal biantennary sugar chain. *Cancer Res.* **59**, 3949–3953 (1999)
- Ide, Y., Miyoshi, E., Nakagawa, T., Gu, J., Tanemura, M., Nishida, T., Ito, T., Yamamoto, H., Kozutsumi, Y., Taniguchi, N.: Aberrant expression of N-acetylglucosaminyltransferase-IVa and IVb (GnT-IVa and b) in pancreatic cancer. *Biochem. Biophys. Res. Commun.* **341**(2), 478–482 (2006). doi:10.1016/j.bbrc.2005.12.208
- Yamashita, K., Koide, N., Endo, T., Iwaki, Y., Kobata, A.: Altered glycosylation of serum transferrin of patients with hepatocellular carcinoma. *J. Biol. Chem.* **264**(5), 2415–2423 (1989)
- Ellis, S.M., Nabeshima, K., Biswas, C.: Monoclonal antibody preparation and purification of a tumor cell collagenase-stimulatory factor. *Cancer Res.* **49**(12), 3385–3391 (1989)
- Polette, M., Gilles, C., Marchand, V., Lorenzato, M., Toole, B., Tournier, J.M., Zucker, S., Birembaut, P.: Tumor collagenase stimulatory factor (TCSF) expression and localization in human lung and breast cancers. *J. Histochem. Cytochem.* **45**(5), 703–709 (1997)
- Wang, S., Li, B., Li, Y., Li, J.: Expression and clinical significance of CD147 and MMP-2 in squamous cell carcinoma and adenocarcinoma of the lungs. *Zhongguo Fei Ai Za Zhi* **14**(9), 710–714 (2011). doi:10.3779/j.issn.1009-3419.2011.09.02
- Suzuki, S., Sato, M., Senoo, H., Ishikawa, K.: Direct cell-cell interaction enhances pro-MMP-2 production and activation in co-culture of laryngeal cancer cells and fibroblasts: involvement of EMMPRIN and MT1-MMP. *Exp. Cell Res.* **293**(2), 259–266 (2004)
- Tang, W., Chang, B.S., Hemler, M.E.: Links between CD147 Function, Glycosylation, and Caveolin-1. *Mol. Biol. Cell* **15**, 4043–4050 (2004)
- Jia, L., Wang, S., Zhou, H., Cao, J., Hu, Y., Zhang, J.: Caveolin-1 up-regulates CD147 glycosylation and the invasive capability of murine hepatocarcinoma cell lines. *Int. J. Biochem. Cell Biol.* **38**(9), 1584–1593 (2006). doi:10.1016/j.biocel.2006.03.019
- Li, H.F., Ling, M.Y., Xie, Y., Xie, H.: Establishment of a lymph node metastatic model of mouse hepatocellular carcinoma Hca-F cells in C3H/Hej mice. *Oncol. Res.* **10**(11–12), 569–573 (1998)
- Jia, L., Wang, S., Cao, J., Zhou, H., Wei, W., Zhang, J.: siRNA targeted against matrix metalloproteinase 11 inhibits the metastatic capability of murine hepatocarcinoma cell Hca-F to lymph nodes. *Int. J. Biochem. Cell Biol.* **39**(11), 2049–2062 (2007). doi:10.1016/j.biocel.2007.05.023

29. Dong, L., Liu, Y., Colberg-Poley, A.M., Kaucic, K., Ladisch, S.: Induction of GM1a/GD1b synthase triggers complex ganglioside expression and alters neuroblastoma cell behavior; a new tumor cell model of ganglioside function. *Glycoconj. J.* **28**(3–4), 137–147 (2011). doi:10.1007/s10719-011-9330-9
30. Thompson, C.C., Ashcroft, F.J., Patel, S., Saraga, G., Vimalachandran, D., Prime, W., Campbell, F., Dodson, A., Jenkins, R.E., Lemoine, N.R., Crnogorac-Jurcevic, T., Yin, H.L., Costello, E.: Pancreatic cancer cells overexpress gelsolin family-capping proteins, which contribute to their cell motility. *Gut* **56**(1), 95–106 (2007). doi:10.1136/gut.2005.083691
31. Lee, G.H., Yan, C., Shin, S.J., Hong, S.C., Ahn, T., Moon, A., Park, S.J., Lee, Y.C., Yoo, W.H., Kim, H.T., Kim, D.S., Chae, S.W., Kim, H.R., Chae, H.J.: BAX inhibitor-1 enhances cancer metastasis by altering glucose metabolism and activating the sodium-hydrogen exchanger: the alteration of mitochondrial function. *Oncogene* **29**(14), 2130–2141 (2010). doi:10.1038/onc.2009.491
32. Suzuki, O., Nozawa, Y., Kawaguchi, T., Abe, M.: Phaseolus vulgaris leucoagglutinating lectin-binding reactivity in human diffuse large B-cell lymphoma and its relevance to the patient's clinical outcome: lectin histochemistry and lectin blot analysis. *Pathol. Int.* **49**(10), 874–880 (1999)
33. Apweiler, R., Hermjakob, H., Sharon, N.: On the frequency of protein glycosylation, as deduced from analysis of the SWISS-PROT database. *Biochim. Biophys. Acta* **1473**(1), 4–8 (1999)
34. Tan, J., D'Agostaro, A.F., Bendiak, B., Reck, F., Sarkar, M., Squire, J.A., Leong, P., Schachter, H.: The human UDP-N-acetylglucosamine: alpha-6-D-mannoside-beta-1,2- N-acetylglucosaminyltransferase II gene (MGAT2). Cloning of genomic DNA, localization to chromosome 14q21, expression in insect cells and purification of the recombinant protein. *Eur. J. Biochem.* **231**(2), 317–328 (1995)
35. Saito, H., Nishikawa, A., Gu, J., Ihara, Y., Soejima, H., Wada, Y., Sekiya, C., Niikawa, N., Taniguchi, N.: cDNA cloning and chromosomal mapping of human N-acetylglucosaminyltransferase V+. *Biochem. Biophys. Res. Commun.* **198**(1), 318–327 (1994)
36. Ihara, Y., Nishikawa, A., Tohma, T., Soejima, H., Niikawa, N., Taniguchi, N.: cDNA cloning, expression, and chromosomal localization of human N-acetylglucosaminyltransferase III (GnT-III). *J. Biochem.* **113**(6), 692–698 (1993)
37. Kumar, R., Yang, J., Larsen, R.D., Stanley, P.: Cloning and expression of N-acetylglucosaminyltransferase I, the medial Golgi transferase that initiates complex N-linked carbohydrate formation. *Proc. Natl. Acad. Sci. U.S.A.* **87**(24), 9948–9952 (1990)
38. Mizuochi, T., Nishimura, R., Derappe, C., Taniguchi, T., Hamamoto, T., Mochizuki, M., Kobata, A.: Structures of the asparagine-linked sugar chains of human chorionic gonadotropin produced in choriocarcinoma. Appearance of triantennary sugar chains and unique biantennary sugar chains. *J. Biol. Chem.* **258**(23), 14126–14129 (1983)
39. Kobata, A.: Structures, function, and transformational changes of the sugar chains of glyco hormones. *J. Cell. Biochem.* **37**(1), 79–90 (1988). doi:10.1002/jcb.240370108
40. Yamashita, K., Totani, K., Iwaki, Y., Takamisawa, I., Tateishi, N., Higashi, T., Sakamoto, Y., Kobata, A.: Comparative study of the sugar chains of gamma-glutamyltranspeptidases purified from human hepatocellular carcinoma and from human liver. *J. Biochem.* **105**(5), 728–735 (1989)
41. Zhao, Y., Li, J., Xing, Y., Wang, J., Lu, C., Xin, X., Geng, M.: N-acetylglucosaminyltransferase V mediates cell migration and invasion of mouse mammary tumor cells 4T07 via RhoA and Rac1 signaling pathway. *Mol. Cell. Biochem.* **309**(1–2), 199–208 (2008). doi:10.1007/s11010-007-9656-6
42. Wang, C., Yang, Y., Yang, Z., Liu, M., Li, Z., Sun, L., Mei, C., Chen, H., Chen, L., Wang, L., Zha, X.: EGF-mediated migration signaling activated by N-acetylglucosaminyltransferase-V via receptor protein tyrosine phosphatase kappa. *Arch. Biochem. Biophys.* **486**(1), 64–72 (2009). doi:10.1016/j.abb.2009.02.005
43. Zhang, H., Meng, F., Wu, S., Kreike, B., Sethi, S., Chen, W., Miller, F.R., Wu, G.: Engagement of I-branching beta-1, 6-N-acetylglucosaminyltransferase 2 in breast cancer metastasis and TGF- $\beta$  signaling. *Cancer Res.* **71**(14), 4846–4856 (2011). doi:10.1158/0008-5472.CAN-11-0414
44. Guan, W., Ban, L., Cai, L., Li, L., Chen, W., Liu, X., Mrksich, M., Wang, P.G.: Combining carbochips and mass spectrometry to study the donor specificity for the Neisseria meningitidis beta1,3-N-acetylglucosaminyltransferase LgtA. *Bioorg. Med. Chem. Lett.* **21**(17), 5025–5028 (2011). doi:10.1016/j.bmcl.2011.04.100
45. Gu, J., Zhao, Y., Isaji, T., Shibukawa, Y., Ihara, H., Takahashi, M., Ikeda, Y., Miyoshi, E., Honke, K., Taniguchi, N.: Beta1,4-N-Acetylglucosaminyltransferase III down-regulates neurite outgrowth induced by costimulation of epidermal growth factor and integrins through the Ras/ERK signaling pathway in PC12 cells. *Glycobiology* **14**(2), 177–186 (2004). doi:10.1093/glycob/cwh016cwh016
46. Yoshida, A., Minowa, M.T., Takamatsu, S., Hara, T., Oguri, S., Ikenaga, H., Takeuchi, M.: Tissue specific expression and chromosomal mapping of a human UDP-N-acetylglucosamine: alpha1,3-d-mannoside beta1, 4-N-acetylglucosaminyltransferase. *Glycobiology* **9**(3), 303–310 (1999)
47. Koyama, N., Miyoshi, E., Ihara, Y., Kang, R., Nishikawa, A., Taniguchi, N.: Human N-acetylglucosaminyltransferase III gene is transcribed from multiple promoters. *Eur. J. Biochem.* **238**(3), 853–861 (1996)
48. Saito, H., Gu, J., Nishikawa, A., Ihara, Y., Fujii, J., Kohgo, Y., Taniguchi, N.: Organization of the human N-acetylglucosaminyltransferase V gene. *Eur. J. Biochem.* **233**(1), 18–26 (1995)
49. Oguri, S., Minowa, M.T., Ihara, Y., Taniguchi, N., Ikenaga, H., Takeuchi, M.: Purification and characterization of UDP-N-acetylglucosamine: alpha1,3-D-mannoside beta1,4-N-acetylglucosaminyltransferase (N-acetylglucosaminyltransferase-IV) from bovine small intestine. *J. Biol. Chem.* **272**(36), 22721–22727 (1997)
50. Kozak, M.: An analysis of 5'-noncoding sequences from 699 vertebrate messenger RNAs. *Nucleic Acids Res.* **15**(20), 8125–8148 (1987)
51. Jia, L., Zhou, H., Wang, S., Cao, J., Wei, W., Zhang, J.: Deglycosylation of CD147 down-regulates Matrix Metalloproteinase-11 expression and the adhesive capability of murine hepatocarcinoma cell HcaF *in vitro*. *IUBMB Life* **58**(4), 209–216 (2006). doi:10.1080/15216540600719580